Appl Phys A (2011) 105:341–345
DOI 10.1007/s00339-011-6612-9

Applied Physics A
Materials Science & Processing

RAPID COMMUNICATION

Cobalt-assisted large-area epitaxial graphene growth in thermal cracker enhanced gas source molecular beam epitaxy

Ning Zhan · Guoping Wang · Jianlin Liu

Received: 28 May 2011 / Accepted: 12 September 2011 / Published online: 28 September 2011

Abstract Large-area epitaxial graphene films were grown on cobalt by thermal cracker enhanced gas source molecular beam epitaxy. Growth conditions including growth temperature and growth time play important roles in the resulting morphology of as-grown films. High-quality graphene films can be achieved in a small growth window. Fast cooling rate was not required in this process due to direct growth mechanism under atomic carbon growth condition. Large-area graphene films with high single-layer and bi-layer coverage of 93% were confirmed by Raman spectroscopy and transmission electron microscopy.

1 Introduction

Graphene has attracted tremendous attention in various fields since it was discovered [1]. A few methods have been implemented to synthesize large-area graphene, such as mechanical exfoliation of graphite [1], graphitization of SiC substrate [2] and chemical vapor deposition (CVD) of carbon on metal substrates [3–8]. In CVD method, various metals including Ni [3–5], Cu [6, 7], and Co [8–10] have been used. Owing to its very small lattice mismatch to graphene [11], Co shall be an ideal substrate. Nevertheless, large-area, high-quality graphene on Co substrates is still a challenge in CVD process. Earlier, as-grown graphene films were either very small (several nanometers, or tens micron by tens micron) or containing inhomogeneous islands [8, 10]. Ago et al. reported large-area graphene on Co/sapphire, which relied on rapid cooling of the sample by pulling out the substrate from the CVD furnace immediately after the growth [12]. Carbon precipitation from Co is responsible for the CVD growth of graphene, however, rapid temperature cooling is not very controllable, leading to the difficulty of controlling the number of graphene layers. To better control the number of graphene layers, traditional direct layer-by-layer growth of graphene on a substrate may be more desirable compared with carbon precipitation. Recently we reported large-area graphene growth on Ni substrate by using thermal cracker enhanced gas source molecular beam epitaxy (GSMBE) [13]. With the introduction of atomic carbon atoms onto Ni substrate, direct epitaxial growth of graphene was achieved at an elevated growth temperature and very fast cooling to suppress the formation of multi-layer is not necessary. In this letter, we report results of graphene films on Co substrates by thermal cracker enhanced GSMBE. It is found that not only high-quality, large-area graphene can be synthesized, but also the morphology of the graphene is better than that grown on Ni substrate. High single-layer and bi-layer coverage of 93% is achieved by precisely controlling growth temperature and time. The mechanism of the graphene growth is tentatively discussed.

2 Experimental details

500 nm Co film was deposited on SiO_2 (300 nm)/Si substrate by electron beam evaporation. The substrate was immediately transferred into a thermal cracker enhanced GSMBE chamber for preventing surface contamination. Hydrogen of 10 sccm (standard cubic centimeters per minute) was input into the chamber during temperature ramping up. After the target temperature was reached, acetylene of 10 sccm was introduced into the chamber through a thermal

N. Zhan · G. Wang · J. Liu (✉)
Quantum Structures Laboratory, Department of Electrical Engineering, University of California, Riverside, CA 92521, USA
e-mail: jianlin@ee.ucr.edu

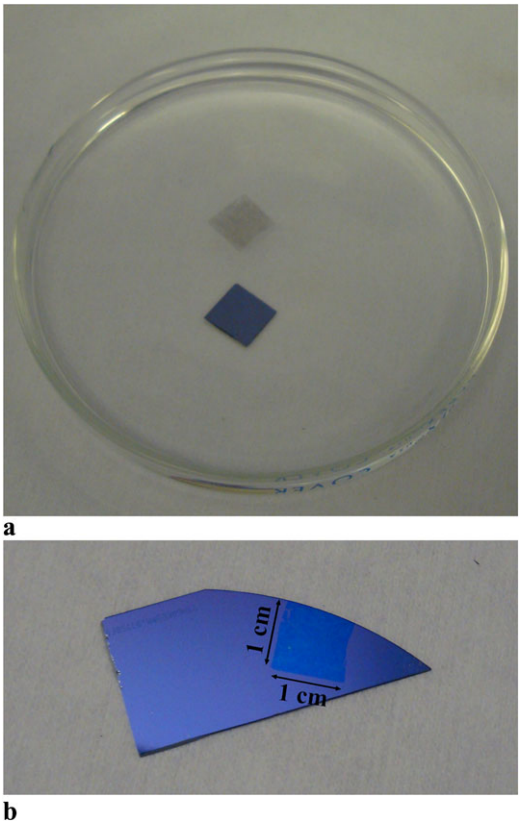

Fig. 1 (**a**) A floating PMMA/graphene after underneath Co film was etched in 5% HCl solution. (**b**) A transferred graphene film on SiO_2(300 nm)/Si substrate

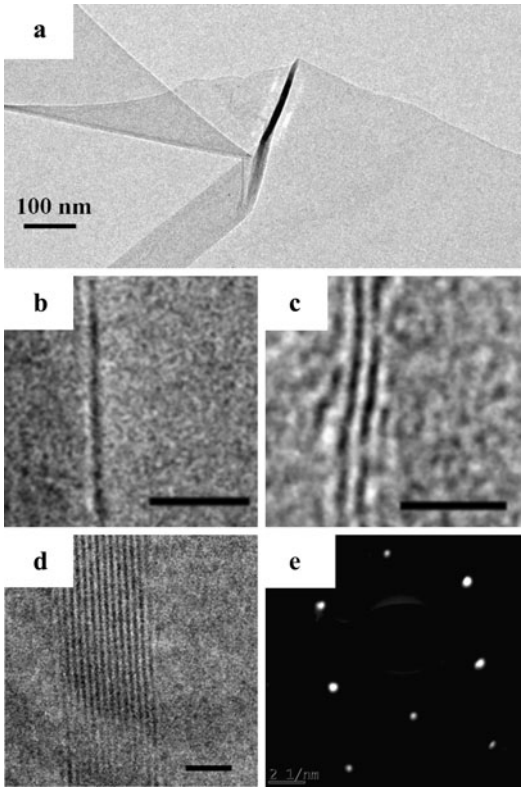

Fig. 2 (**a**) Top-view TEM image of the graphene film. (**b**), (**c**) and (**d**) are TEM cross-sectional images of single-layer, bi-layer and multi-layer graphene, respectively (the *scale bar* is 2 nm). (**e**) Diffraction pattern of as-grown sample

cracker, which operates at a temperature of 1200∼1300°C, to provide atomic carbon beam onto the substrate for graphene growth. The sample was cooled to room temperature after growth.

To transfer as-grown graphene films to desired substrates, polymethyl-methacrylate (PMMA) was spin-coated on graphene/Co/SiO_2/Si substrate. After baked at 180°C for 2 minutes, the whole sample was dipped into a mild HCl solution (5%) and the Co film was etched, which usually took 12 hours. After the Co film was etched away, PMMA/graphene film floating inside the solution was lifted by the same SiO_2/Si substrate slowly. Acetone was used to dissolve the PMMA layer after transferring PMMA/graphene to a desired substrate.

High-resolution Philips CM300 transmission electron microscope (TEM) with electron gun voltage of 300 kV was used to characterize as-grown films. The Raman spectrum was measured at room temperature with laser wavelength of 532 nm and power of 0.3 mW.

3 Results and discussion

Figure 1(a) shows the PMMA/graphene film floating inside solution after the metal substrate was etched. This sample was grown at a temperature of 950°C. After 4-minute carbon growth with acetylene flow rate of 10 sccm, the sample was cooled at a rate of 10°C/min. As seen from the figure, the PMMA layer effectively protects the intactness of the as-grown film. After the PMMA layer was dissolved, the graphene film still maintained a continuous form, being strongly attached to the SiO_2/Si substrate (Fig. 1(b)). The size of the film is 1 cm × 1 cm, which is limited by the size of the substrate holder in the GSMBE system.

Figure 2(a) shows a top-view TEM image of the film. Except the areas where the graphene films fold up with each other, very even brightness of the film is evident, which indicates good morphology of the as-grown film. Figures 2(b)–(d) show cross-sectional TEM images of single-layer, bi-layer and multi-layer graphene, respectively, which exist in the same sample. The interlayer distance of 3.4 Å obtained by fast Fourier transform agrees with that of graphite. A clear hexagonal shape diffraction pattern from most part of the film confirms good crystalline of the as-grown film (Fig. 1(e)).

Raman spectroscopy is a very powerful tool for characterizing carbon nanostructures because of its sensitivity to carbon sp^2 and sp^3 bonds. Therefore, the position of G peak (∼1580 cm^{-1}), profile of 2D peak (∼2700 cm^{-1}) and ratio

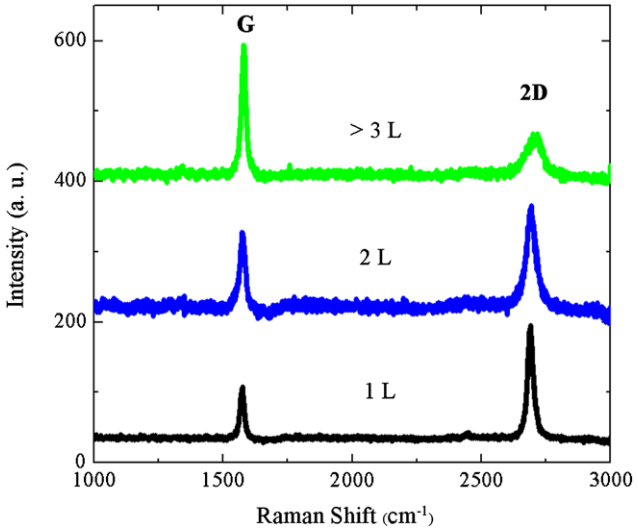

Fig. 3 Raman spectra of graphene film grown at 950°C

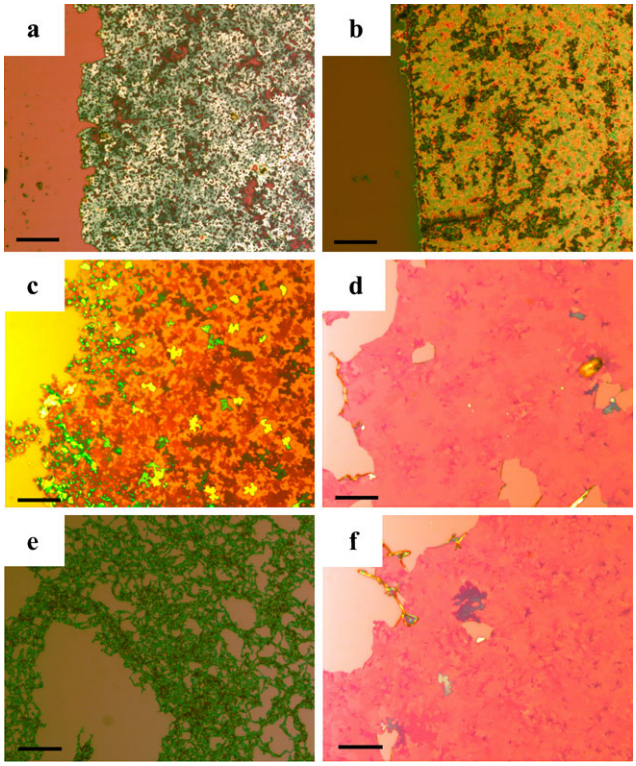

Fig. 4 Optical microscopy images of as-grown graphene films transferred on 300 nm SiO_2/Si substrate with different growth temperatures, (**a**) 800°C, (**b**) 850°C, (**c**) 900°C, (**d**) 950°C, (**e**) 1000°C. The *scale bar* is 50 μm. Cooling rate of 10°C/min was used for these five samples. (**f**) Graphene film synthesized at the same growth condition as (**d**) except using an average cooling rate of 200°C/min

of intensities between these two peaks (I_G/I_{2D}) change evidently with the thickness of graphene films exfoliated from graphite. For epitaxial graphene films, however, the G peak position can also be easily changed as a result of the interface strain between as-grown graphene films and SiO_2 substrate during transferring process [14]. In addition, as-grown graphene usually does not have strict AB Bernal stacking between each layer, leading to insignificant dependence of evolution of 2D peak on its thickness [13, 15]. Reina et al. [5] found a quantitative relation between the intensity ratio of G peak and 2D peak (I_G/I_{2D}) and number of layers for epitaxial graphene; ratios of <0.5 and $0.5\sim1$ correspond to single- and bi-layer, respectively. For higher ratio (>1.8), the films are either multi-layer graphene or graphite. Figure 3 shows Raman spectra of the graphene grown at 950°C, which was already transferred to SiO_2/Si substrate. Three curves were taken from three typical positions that exhibit different optical contrast under an optical microscope. The intensity ratios I_G/I_{2D} for the curves from bottom to top are 0.45, 0.73 and 3.17, corresponding to single-layer, bi-layer and multi-layer graphene, respectively. 93% single-layer and bi-layer coverage can be obtained by Raman mapping and color histogram in the optical microscopy image, which is much higher than that of graphene grown on Ni in CVD [3, 5]. No detectable D band ($\sim$1350 cm^{-1}) was observed in single-layer and bi-layer areas, indicating good quality of the as-grown film. A very small D peak can be found in multi-layer region, which may be due to the formation of dislocations at boundaries.

Figures 4(a)–(e) show optical microscopy images of graphene films transferred on SiO_2/Si substrates. These films were grown at the temperatures from 800°C to 1000°C, respectively. All other growth conditions were kept the same including a cooling rate of 10°C/min, a growth pressure of 3×10^{-3} Torr, a flow rate of 10 sccm, and a growth time of 4 minutes. As seen from Figs. 4(a)–(b), very high color contrast between graphene films (right side of the images) and SiO_2 (left side of the images) can be observed, indicating the growth of graphite, which is also confirmed by Raman scattering measurements (not shown here). The as-grown films become thinner with the increase of the temperature, few-layer graphene with only small percentage (Fig. 4(c)) emerges at 900°C. As the temperature reaches 950°C, uniform and continuous graphene films dominated by single-layer and bi-layer finally grow on the substrate (Fig. 4(d)). Some holes in the image are mainly due to inadvertent physical damage during transferring process. Nevertheless, further increase of temperature to 1000°C leads to graphene with porous net morphology (Fig. 4(e)). Therefore, the growth temperature is critical to obtain good quality of graphene films in thermal cracker enhanced GSMBE. As-grown films could be either thick graphite or porous net if the temperature would be lower or higher than the optimal one, which is 950°C in this case.

Graphene grown by carbon precipitation mechanism in CVD method typically requires a rapid cooling rate (160°C/min or 600°C/min [3, 4, 16]) to suppress the forma-

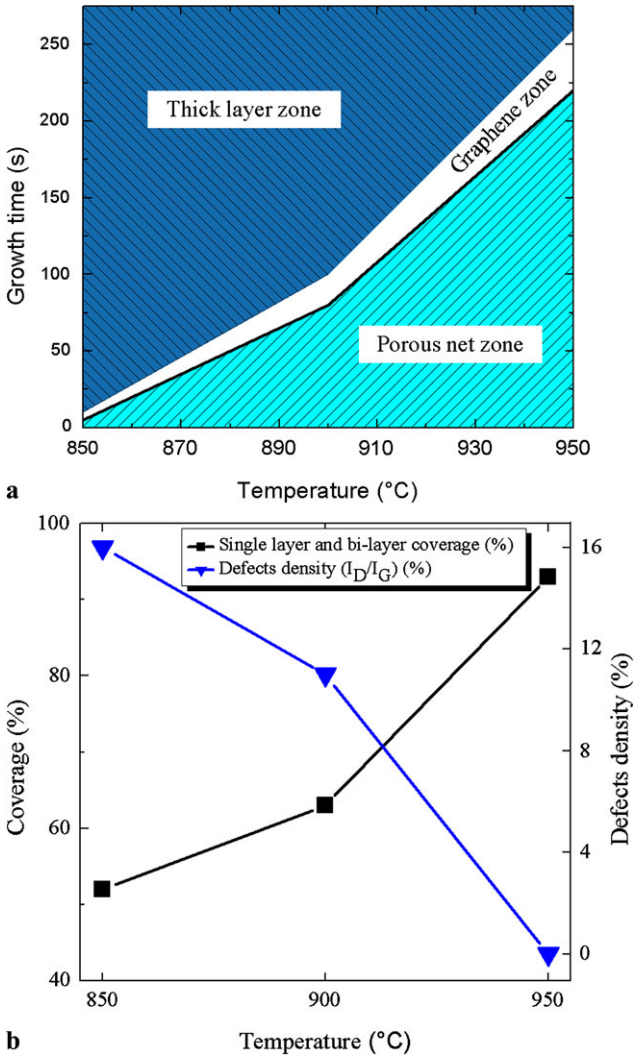

Fig. 5 (**a**) Diagram of the morphology of as-grown films versus growth time at different temperatures. (**b**) Single-layer and bi-layer coverage and defects density dependence on growth temperature

tion of multi-layer graphene. In thermal cracker enhanced GSMBE, the situation is different. Figure 4(f) shows an optical microscopy image of the graphene sample, which was grown at a cooling rate of 200°C/min from 950°C. All other growth conditions for this sample are the same as that of the sample shown in Fig. 4(d), in which a cooling rate of only 10°C/min was used. No observable difference can be found between Figs. 4(d) and 4(f), which means different cooling rates do not result in a different number of layers in graphene growth. This result implies that the growth mechanism is direct epitaxial carbon growth in thermal cracker enhanced GSMBE rather than carbon precipitation as observed in CVD, which is further confirmed by the growth-time dependence as described in the following.

The growth-time dependence was carried out at the temperatures of 850°C, 900°C and 950°C, respectively (Fig. 5(a)). At each temperature, graphene films started with porous net structures as the growth was short; became continuous films as the growth time was moderate; and evolved to thick graphite as the growth was long. Since the cooling rate used in each growth is the same at 10°C/min, this result is the direct evidence of direct carbon growth on Co. For quantitative analysis purpose, the thick film with single-layer and bi-layer coverage of less than 50% is defined as thick layer, and the film with holes occupying more than 50% of the whole area is defined as porous net. Figure 5(a) shows this quantitative dependence at different temperatures. The major part of the image is occupied by "thick layer zone" and "porous net zone", graphene is formed only in a very small growth window. This growth window is only 5 seconds at 850°C, and it becomes bigger with the increase of temperature, reaching 40 seconds as temperature is 950°C.

Figure 5(b) shows single-layer and bi-layer coverage, and corresponding defects density (Raman peak intensity ratio I_G/I_{2D}) as a function of growth temperature. The coverage of films grown at 850°C is only 52%, and increases to 63% at 900°C, and 93% at 950°C; while the I_G/I_{2D} ratio decreases from 16% at 850°C, to 11% at 900°C and further to negligible percentage at 950°C. Low temperature causes insufficient thermal energy provided by substrate, which decreases the diffusion length of carbon atoms on the Co surface. The areas with more nucleation centers on grain boundaries easily keep absorbing carbon atoms and forming graphene. In the mean time, other areas have much less carbon to grow, which brings about unevenness and also lots of defects between different areas. With the increase of the substrate temperature, carbon atoms have larger diffusion length and more freely migrate around Co substrate. Fewer defects are observed because of more evenness across different areas. In addition, flatter Co surface may be generated at higher temperature, leading to more uniform first-layer graphene growth.

Finally, the Co-assisted graphene growth in thermal cracker enhanced GSMBE can be described as follows. During carbon growth in GSMBE, once acetylene molecules are broken by thermal cracker, atomic carbon beams form and impinge onto Co substrate. The substrate then adsorbs incoming carbon atoms to form graphene. At initial stage when there are not enough incoming carbon atoms, boundaries and surface defects act as nucleation centers, having priority to absorb carbon atoms and form graphene film, which explains why short-time growth always brings about porous net. Once monolayer graphene covers Co surface, further carbon beam acts as source for epitaxial growth on existing layer, leading to thick layer growth. Besides the adsorption process, the desorption process also plays an important role in graphene growth. As the desorption coefficient increases at higher temperature, carbon atoms are harder to absorb by Co to form graphene, leading to thinner carbon

growth and eventually porous net morphology at 1000°C, which was observed in Figs. 4(a)–(e).

4 Conclusions

Large-area epitaxial graphene films were achieved on Co substrates in thermal cracker enhanced GSMBE system. Clear TEM diffraction pattern and lacking D peak in Raman spectra indicate the high quality of as-grown films. The single-layer and bi-layer coverage of 93% was achieved at an optimized temperature of 950°C. A narrow growth-time window was found for different growth temperatures. Carbon absorption and desorption phenomena were responsible for temperature-dependent and growth-time-dependent graphene morphology. Direct epitaxial growth mechanism was confirmed through temperature cooling rate and growth-time-dependent experiments. These studies suggest that thermal cracker GSMBE can be promising in growing large-area graphene on Co substrates.

Acknowledgement The authors would like to thank the Center of Nanomaterials and Nanodevices funded by the Defense Microelectronics Activity (DMEA) under the agreement number H94003-10-2-1003.

References

1. K.S. Novoselov, A.K. Geim, S.V. Morozov, D. Jiang, Y. Zhang, S.V. Dubonos, I.V. Grigorieva, A.A. Firsov, Science **306**, 666 (2004)
2. C. Berger, Z. Song, X. Li, X. Wu, N. Brown, C. Naud, D. Mayou, T. Li, J. Hass, A.N. Marchenkov, E.H. Conrad, P.N. First, W.A. de Heer, Science **312**, 1191 (2006)
3. S.J. Chae, F. Güne, K.K. Kim, E.S. Kim, G.H. Han, S.M. Kim, H.-J. Shin, S.-M. Yoon, J.-Y. Choi, M.H. Park, C.W. Yang, D. Pribat, Y.H. Lee, Adv. Mater. **21**, 2328 (2009)
4. K.S. Kim, Y. Zhao, H. Jang, S.Y. Lee, J.M. Kim, K.S. Kim, J.-H. Ahn, P. Kim, J.-Y. Choi, B.H. Hong, Nature **457**, 706 (2009)
5. A. Reina, X. Jia, J. Ho, D. Nezich, H. Son, V. Bulovic, M.S. Dresselhaus, J. Kong, Nano Lett. **9**, 30 (2009)
6. X. Li, Y. Zhu, W. Cai, M. Borysiak, B. Han, D. Chen, R.D. Piner, L. Colombo, R.S. Ruoff, Nano Lett. **9**, 4359 (2009)
7. X. Li, C.W. Magnuson, A. Venugopal, J. An, J.W. Suk, B. Han, M. Borysiak, W. Cai, A. Velamakanni, Y. Zhu, L. Fu, E.M. Voge, E. Voelk, L. Colombo, R.S. Ruoff, Nano Lett. **10**, 4328 (2010)
8. D. Eom, D. Prezzi, K.T. Rim, H. Zhou, M. Lefenfeld, S. Xiao, C. Nuckolls, M.S. Hybertsen, T.F. Heinz, G.W. Flynn, Nano Lett. **9**, 2844 (2009)
9. J. Vaari, J. Lahtinen, P. Hautojarvi, Catal. Lett. **44**, 43 (1997)
10. H. Ago, I. Tanaka, C.M. Orofeo, M. Tsuji, K.-I. Ikeda, Small **11**, 1226 (2010)
11. R.W.G. Wyckoff, *The Structure of Crystals*, 2nd edn. (The Chemical Catalog, New York, 1931)
12. H. Ago, Y. Ito, N. Mizuta, K. Yoshida, B. Hu, C.M. Orofeo, M. Tsuji, K.-I. Ikeda, S. Mizuno, ACS Nano **4**, 7407 (2010)
13. N. Zhan, M. Olmedo, G. Wang, J. Liu, Carbon **49**, 2046 (2011)
14. M.S. Dresselhaus, A. Jorio, M. Hofmann, G. Dresselhaus, R. Saito, Nano Lett. **10**, 751 (2010)
15. L.M. Malard, M.A. Pimenta, G. Dresselhaus, M.S. Dresselhaus, Phys. Rep. **473**, 51 (2009)
16. D.I. Son, T.W. Kim, J.H. Shim, J.H. Jung, D.U. Lee, J.M. Lee, W.I. Park, W.K. Choi, Nano Lett. **10**, 2441 (2010)